PROCESSING OF MSG-1 SEVIRI DATA IN THE THERMAL INFRARED - ALGORITHM DEVELOPMENT WITH THE USE OF THE SPARC2004 DATA SET

A.S.M. Gieske[(1)], J. Hendrikse [(1)], V. Retsios [(1)] , B. van Leeuwen [(1)] , B.H.P. Maathuis[(1)] , M. Romaguera[(2)], J.A. Sobrino[(2)], W.J. Timmermans[(1)], Z. Su[(1)]

[(1)] *International Institute for Geo-Information Science and Earth Observation (ITC), Enschede, The Netherlands, gieske@itc.nl*

[(2)] *Department of Thermodynamics, University of Valencia, Spain*

ABSTRACT

The processing of HRIT wavelet compressed data, received at ITC with a standard size dish, is discussed. Specifically a 14 day full disk image time series was generated with the aim of producing a data set of the Iberian Peninsula to support the ESA/SPARC 2004 field campaign. Software was developed for the efficient extraction of a image time series, which is both geocoded and radiometrically corrected. Improvements to the SEVIRI processing toolbox are discussed. To be able to generate Land Surface Temperatures, simple atmospheric corrections are being developed, using split window techniques and fast approximations to MODTRAN. Finally, total ozone content is determined through application of the method by Drouin and Karcher, with the use of p-T atmospheric profiles from the ECMWF (MARS) archives and MODIS level 2 products.

1. INTRODUCTION

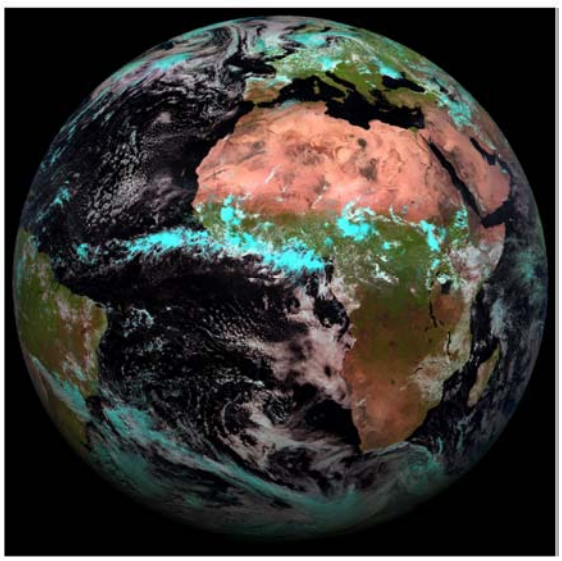

Fig. 1 The figure shows a MSG-1/SEVIRI image of July 10, 2004, 1200 hrs as a False Color Composite of bands 1, 2 and 3 (EUMETSAT, 2004).

The SEVIRI data are received from MSG-1 by EUMETSAT at Darmstadt (Germany). They are then processed and uplinked to HOTBIRD-6 in wavelet compressed HRIT format. From there the images can be received with a standard dish receiving system (Fig. 2) in the Eumetcast Ku band. At ITC they are archived in compressed form on external drives linked to the ITC network, and accessible through ordinary PCs.

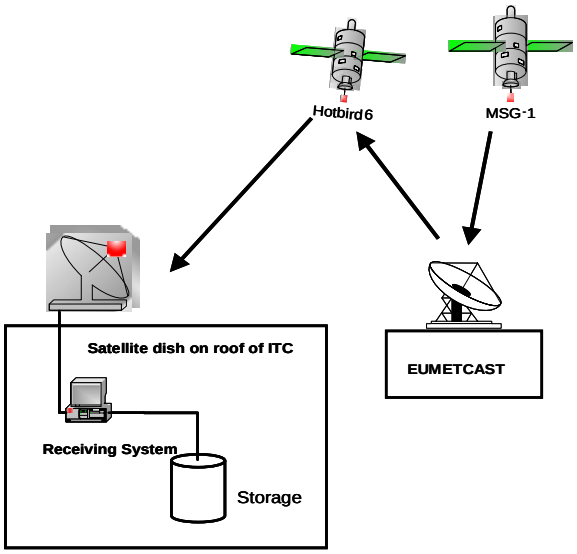

Fig. 2 Re-broadcasting of MSG-1 data after processing by EUMETSAT. Image data are received at ITC from HOTBIRD using a standard dish (EUMETCAST, Ku-band).

The processing of the images for Earth Observation application purposes requires a number of pre-processing steps that are in principle straightforward. However, there are many practical difficulties that create problems in the implementations. For this reason, detailed calculations have been summarized in the appendices of this paper. The following steps need to be taken:

- wavelet decompression
- geometric coding
- solar zenith/azimuth angle calculations
- satellite view/azimuth angle calculations
- radiometric calibration

Documentation to implement the steps is provided by Eumetsat in [1], [2], [3] and [4]. However, the information is scattered, and no single Algorithm Theoretical Base Document is available. Therefore it was decided at ITC, to improve the accessibility of the imagery to the applications and create in-house software that would be fast and efficient in the generation and extraction of image time series [5].

In the first step, wavelet decompression, use is made of the compiled software provided under licence by Eumetsat [1]. The geometric coding, the solar zenith and view angle calculations are discussed in the next sections. The radiometric top-of-the-atmosphere calibration is described after that.

Two applications in the thermal domain 8-14 μm are briefly discussed as examples (channels 7-11, as in Table 1 below). First, the determination of Land Surface Temperatures (LSTs) as validated in the SPARC2004 field campaign is reviewed [6], [7], together with atmospheric correction procedures. See also the reports on LST in this volume. Finally, a short discussion is given of the total ozone method [8] as applied in this case, where use is made of the ECMWF (MARS) p-T atmospheric profiles, together with the MODIS level 2 p-T profiles.

Table 1. The 12 channels of (MSG-1) SEVIRI. This paper concentrates on channels 7-11 in the Thermal Infrared (TIR) (source www.eumetsat.de).

Channel no.		Characteristics of spectral band (μm)			Main gaseous absorber or window
		λ_{con}	λ_{min}	λ_{max}	
1	VIS0.6	0.635	0.56	0.71	Window
2	VIS0.8	0.81	0.74	0.88	Window
3	NIR1.6	1.64	1.50	1.78	Window
4	IR3.9	3.90	3.48	4.36	Window
5	WV6.2	6.25	5.35	7.15	Water vapor
6	WV7.3	7.35	6.85	7.85	Water vapor
7	IR8.7	8.70	8.30	9.10	Window
8	IR9.7	9.66	9.38	9.94	Ozone
9	IR10.8	10.80	9.80	11.80	Window
10	IR12.0	12.00	11.00	13.00	Window
11	IR13.4	13.40	12.40	14.40	Carbon dioxide
12	HRV	Broadband (about 0.4 – 1.1)			Window/water vapor

3. SOLAR ZENITH AND SATELLITE VIEW ANGLES

The problem of determining the solar zenith and azimuth angle as a function of time and geodetic latitude ϕ, is well known and has been solved in many different ways, e.g. [9] describes the astronomical series required to determine the zenith angle. The SEVIRI Processing Toolbox [4] gives another method. Both these methods are so-called "low-precision" because their precision is in the order of 1 minute. If higher accuracy is desired then [10] gives accurate astronomical methods (1 second). Note that in this case the perturbations due to the Earth-Moon system and the other planets have to be taken into account together with atmospheric refraction effects.

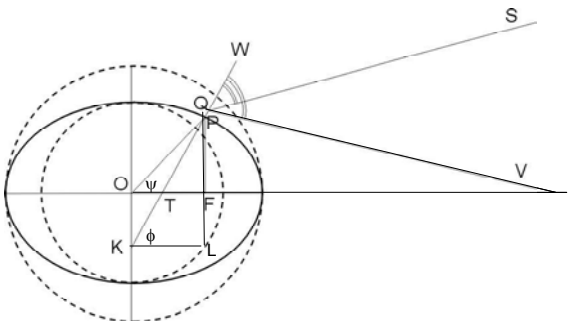

Fig. 3 Diagram showing solar (SQW) and satellite zenith (VQW) angles.

The satellite view angle (angle VQW in Fig. 3) poses a more challenging problem. After analysis it was shown that there may be a slight error in [4] in the order of 0.2^0. Moreover, the analysis also showed that it is perhaps also possible to improve the efficiency of the algorithm given in [4]. The alternative method is discussed in Appendix A for both view and azimuth angles.

4. GEOMETRIC CODING AND RADIOMETRIC CALIBRATION

The problem is to relate the pixel position in terms of row and column number (x,y) to the geodetic coordinates (λ,ϕ) and vice versa. It is important to realize that the pixel position (x,y) in the image corresponds to angles in x and y direction because of the scanning characteristics of the SEVIRI instrument. Moreover, the compressed HRIT image is subdivided into a number of segments where each file contains the necessary geocoding information. The software therefore has to reassemble the full disk Earth image. The projection formulae are given in Appendix B. It was found that the geocoding accuracy is typically in the order of 1 pixel (3km at the subsatellite point). However, in the analysis of image time series it was also noted that jumps sometimes do occur.

A special case is Channel 12 the High Resolution Visible Channel (Table 1). Its resolution is 1km at subsatellite point. The HRV image is composed of two main segments: Europe and the eastern part of Africa. In the near future the African segment will be "sliding" along with the sun position, so this will require adaptation of the software (source: www.eumetsat.de). The geocoding accuracy for the HRV was found to be in the order of several pixels. Moreover, it appears the image is slightly warped and the error therefore does not take the form of a simple translation. Users requiring subpixel accuracy for the HRV channel should take a refining second geocoding step using local ground information.

The radiometric conversion procedure was compiled from [1], [2], [3] and [4] together with information from the EUMETSAT website and is summarized in Appendix C. For radiometric calibration of the 12 bands offsets and gains need to be retrieved from the HRIT compressed file headers. Table 1 (Appendix C below) in columns 2 and 3 shows some typical values obtained for the image of Aug. 5, 2004, 1200 hrs. Unit conversion is a recurrent problem for many users. In order to convert the units from $mWm^{-2}sr^{-1}(cm^{-1})^{-1}$ into $Wm^{-2}sr^{-1}\mu m^{-1}$ the values for each channel have to be multiplied with $10/\lambda_0^2$ where λ_0 is the central wavelength in μm.

5. LST RETRIEVAL AND ATMOSPHERIC CORRECTION

Figure 4 below shows a comparison of Land Surface Temperatures derived from MSG-1 and AHS/INTA on one hand and the field data as reported by [6], [7] and [14] on the other hand. The MSG/SEVIRI data was atmospherically corrected by the split window technique described in [7], while the AHS/INTA hyperspectral data was atmospherically corrected with MODTRAN4. The MSG derived values correspond very well to the average temperatures found in the field during the day, i.e. between those of bare soil and air. The minimum temperatures during the night are in close agreement.

Work is under way to also apply the simple approximation to MODTRAN derived by [12] to the SEVIRI data. The general relation for radiances is as follows:

$$L_{\lambda,surf} = \frac{L_{\lambda,sensor} - L_{\lambda,\uparrow}}{\tau_\lambda} - (1-\varepsilon_\lambda) L_{\lambda,\downarrow} \quad (1)$$

To obtain the surface leaving radiance, the following three atmospheric parameters need to be determined: upwelling radiance, downwelling radiance and transmissivity.

Downwelling radiance is approximated as

$$L_{\lambda,\downarrow} = 1.744 * L_{\lambda,\uparrow}^{0.841} \quad (2)$$

The upwelling radiance and transmissivity are taken as simple functions of the atmospheric pressure, temperature and humidity in accordance with [12]. The balloon radiosoundings have provided these data.

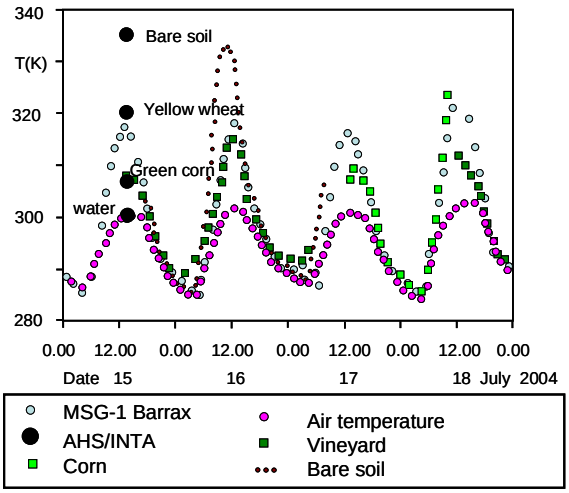

Fig. 4 Land Surface Temperature determined by SEVIRI, validated against Barrax, SPARC2004 field data after [6] and [7].

5. OZONE ALGORITHM

Atmospheric ozone data have been and are collected by a great number of satellites: GOME, TOMS, OMI, NOAA/HIRS, MODIS and SCIAMACHY. However, the 9.7 μm SEVIRI ozone absorption band , also offers excellent possibilities to monitor atmospheric content at time intervals of 15 minutes. EUMETSAT is developing its ozone monitoring capacity as a Satellite Application Facility (SAF) [8].

The SPARC2004 dataset can in principle be used for validation of the MSG ozone algorithm, because direct ozone measurements were taken during the campaign with a MicrotopsII instrument [13] and radio sounding data on p-T are also available.

The ozone procedure adapted from [8] is shown in Figure 5. Three types of data are required:

- MSG-temperature bands (bands 7 to 11) where channel 8 is the ozone absorption band
- The solar zenith and satellite view angles (as described in section 3)
- The pressure and temperature profiles of the atmosphere.

3

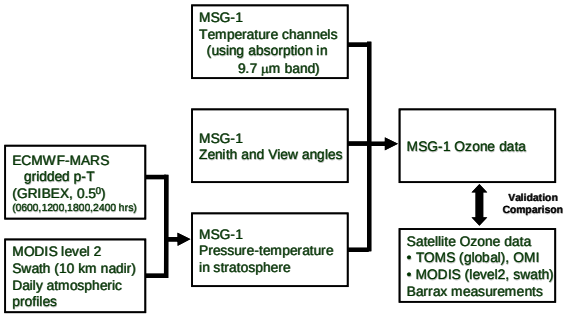

Fig. 5. MSG-1 Ozone Algorithm using archived Pressure-Temperature relations adapted from [8].

Two sources for areal atmospheric p-T depth distributions were tried:

- The ECMWF (SARA) archive Gribex data (0.5 degree resolution) at 4 different times during the day (0600, 1200, 1800 and 2400 hrs). Fig. 6 shows an example of the p-T distribution at 1000 hPa for Europe

- The MODIS level 2 daily atmospheric p-T profiles with a resolution of 10 km at nadir. This data is in so-called swath type format and needs to be reprojected to be of any use. Fig. 7 shows an example of such data for the Iberian Pensinsula.

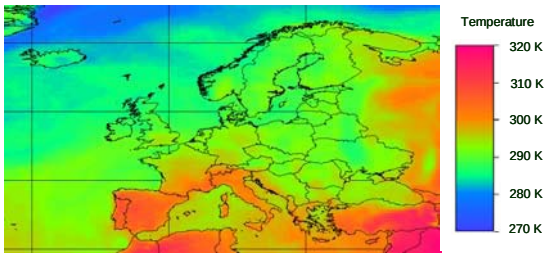

Fig. 6. ECMF MARS Archive p-T Relation for Europe. The figure shows the temperature at 1000 hPa (July 15, 2004, 1200 hrs UTC).

Fig. 8 shows a comparison between the p-T relation obtained by a radio sounding and the corresponding relation from the ECMWF archive. The curves are remarkably close. Diurnal changes only occur near the surface, while in the stratosphere the p-T relation remained constant during that day. Work is being carried out to complete the analysis for both ECMWF and MODIS data for the Iberian Peninsula during June, July and August , and then apply the Karcher ozone algorithm [8].

Finally, Fig. 9 shows the difference in channel 8 (9.7 μm) absorption when AHS/INTA and MSG/SEVIRI are compared. The AHS/INTA sensor flies below most of the stratospheric ozone (Fig. 10) and hence is not affected by the ozone. For the atmospheric correction of the AHS/INTA we would only need to take the water vapour into account, whereas for atmospheric correction of the MSG in the range of 8-14 μm both water vapour and ozone are important.

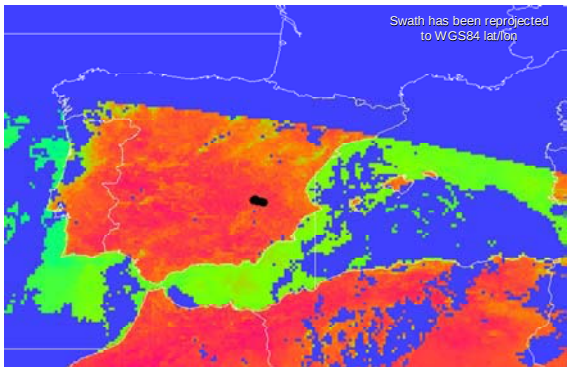

Fig. 7. MODIS level 2, swath reprojected to WGS84 latitude/longitude, atmospheric profile product p-T relation at 20 levels (the data of July 18, 2004, 1100 hrs is shown here).

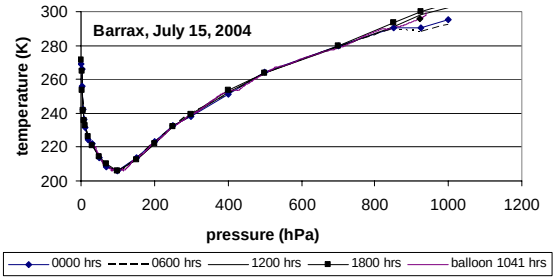

Fig. 8. Pressure-temperature relations from ECMWF (MARS) for 4 times during July 15 2004 compared with Barrax balloon radio soundings of the same day.

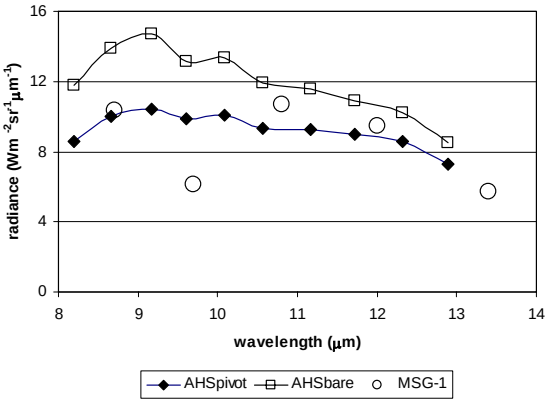

Fig. 9. Comparison of SEVIRI and AHS TIR spectra over Barrax. The absorption of radiation in the MSG ozone (9.7 μm) band is clear, while absorption in this

band does not occur because the airplane flies below the ozone layer (see also Fig. 10).

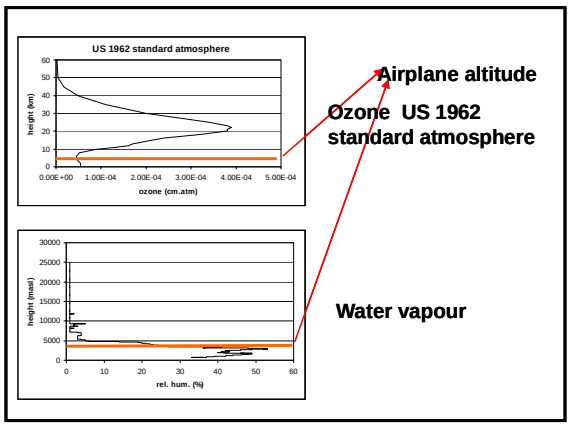

Fig. 10 The figure shows an ozone profile (US 1962) and a radio sounding of water vapour. It is clear that the AHS/INTA airplane flies above most of the water vapour and below most of the ozone.

6. DISCUSSION

Software was developed at ITC to facilitate the processing of MSG/SEVIRI HRIT compressed imagery. During the development extensive use was made of [1], [2], [3] and [4]. However, the discovery of a few small programming errors prompted a new analysis and led to a more efficient approach to the determination of satellite view and zenith angles. It seems advisable to develop a consistent and systematic Algorithmic Theoretical Base Document.

For atmospheric correction of the thermal bands, water vapour and ozone content appear the most important parameters. Use can be made of the split window technique developed by [7] and [14] or by the method of [12]. The ozone content can be inferred from the absorption around 9.7 μm, using ancillary information from e.g. ECMWF or MODIS products. Similar MSG/SEVIRI based methods are available for water vapour and aerosols. So the information can be not only be used for (vicarious) correction of the SEVIRI images themselves but also for atmospheric correction of imagery from other platforms.

7. REFERENCES

1. Eumetsat, *LRIT/HRIT Global Specification*, CGMS 03, Darmstadt, German, 1999.

2. Eumetsat, *MSG Ground Segment LRIT/HRIT Mission Specific Implementation*, MSG/SPE/057, Darmstadt, Germany, 2001a.

3. Eumetsat, *Meteosat Second Generation, Level 1.5 Image Data Format Description*. EUM/MSG/ ICD/105, 2001b.

4. Govaerts, Y. and Clerici, M. 2004. *Seviri Toolbox* (SPT Version 2.1), Eumetsat, Darmstadt, German, 2004.

5. Retsios,V., Maathuis, B.H.P., Gieske, A.S.M., van Leeuwen, B., Hendrikse, J.H.M. and Koolhoven, W., Implementation of a GDAL driver for reading MSG satellite images, *First Holland Open Software Conference, 30 - 31 May 2005*, Amsterdam, The Netherlands, 2005.

6. Romaguera, M., Sobrino, J.A., Gieske, A., Su, Z, and Soria, G. Surface temperature estimation from Meteosat8/SEVIRI data, Algorithms and Validation, *Proc. Symp. China*, 2005.

7. Sobrino, J.A. and Romaguera, M., Land surface temperature retrieval from MSG1-SEVIRI data, *Remote Sensing of Environment*, 92, 247-254. 2004.

8. Drouin, A. and Karcher F. High Resolution Ozone Column derived from SEVIRI 9.7 Ozone Channel. *Proc. Second MSG RAO Workshop*, 9-10 Sept. 2004, Salzburg, Austria, 2004

9. Iqbal, M. *An Introduction to Solar Radiation*, Academic Press, New York, pp389, 1983.

10 Montenbruck, O. and T. Pfleger. *Astronomy on the Personal Computer (4th Ed)*. Springer, Berlin, pp 293, 2005.

11. Kaula, W.M., *Theory of Satellite Geodesy*. Dover Publications, Inc, Minneola, New York, pp 124, 2000.

12. French, A.N., Norman, J.M., and Anderson, M.C. A simple and fast atmospheric correction for space borne remote sensing of surface temperature, *Remote Sensing of Environment*, 87, 326-333, 2003.

13. Molero, F., Pujadas M. , Gómez-Amo, J.L., Estellés, V., Sañudo, E., Utrillas, M.P., Martínez-Lozano, J.A., Fortea, J.C., and Guanter, L. (this volume) Characterization of the atmosphere in SPARC: Ground based measurements of columnar and vertically-resolved atmospheric constituents. ESA/SPARC2004 Proceedings, 2005.

14. Sobrino, A., Jiménez-Muñoz, J.C., Sòria, G., Gómez, M. , Zaragoza, M., Romaguera, M., Cuenca, J. and Julián, Y. (this volume) Thermal Measurements in the framework of SPARC. ESA/SPARC2004 Proceedings, 2005.

APPENDIX A SATELLITE VIEW/AZIMUTH ANGLES

The length of the two axes of the ellipsoid is assumed to be in accordance with the WGS84 model: the equatorial radius a (or r_{eq}) is 6378.1370 km, whereas the polar radius b (or r_{pol}) is assumed to be 6356.7523 km. The distance dv of the geostationary satellite is determined in accordance with Kepler's 3rd Law as 42142.5833 km. This distance may vary slightly as the orbit is not a perfect circle and orbit corrections are made on a regular basis.

The position Q of an observer (pixel) on Earth (see Fig. 3, main text) is determined as follows

$$x = (N+h)\cos\varphi\cos\lambda \tag{1}$$

$$y = (N+h)\cos\varphi\sin\lambda \tag{2}$$

$$z = \left[\left(b^2/a^2\right)N + h\right]\sin\varphi \tag{3}$$

where ϕ is the latitude, λ longitude, h the height above the ellipsoid and parameter N is defined as

$$N = \frac{a}{\sqrt{1-e^2\sin^2\varphi}} \tag{4}$$

where excentricity e is defined as

$$e^2 = 1-\frac{b^2}{a^2} \tag{5}$$

Fig. 3 shows a diagram of the main parameters and distances. The point Q lies on the line KP, and not on the line OP which connects the centre of the Earth with P. The geodetic latitude ϕ is defined by the angle PKL, whereas the geocentric latitude ψ is defined by angle POT. The parameter N is in fact the length of vector KP.

The distance D from Q to the centre of the Earth is given by

$$D = \sqrt{x^2+y^2+z^2} \tag{6}$$

The line KPQ determines the vertical to the Earth's surface at the observer Q, and the direction of this line has to be taken as the local nadir. The solar zenith angle is defined as the acute angle (SQW) between the lines SQ and KW, where S represents the sun (see Fig. 3). Similarly, if the satellite is represented by V, then the satellite zenith angle is the acute angle (VQW) between KQ and QV.

The entire procedure is best carried out with rotation matrices [10], [11]. This leads to a faster and simpler algorithm than the one presented by [4]. First, the geocentric vector ***OQ*** is defined as in Eqns 1-4. The vector ***OV*** is pointing from the Earth's centre to the satellite. The vector ***QV***=***OQ***-***OV*** is then the vector pointing from the observer (Q) to the satellite (V). We now need a rotation from the Earth's geocentric coordinate system to the coordinate system in the observer plane, i.e. a plane tangential to the Earth's ellipsoidal surface in point Q. This rotation depends on ϕ and λ. When the positive x direction is chosen to the North, vector ***U*** in the new coordinate system is then equal to

$$\vec{u} = \begin{pmatrix} -\sin\varphi\cos\lambda & -\sin\varphi\sin\lambda & \cos\varphi \\ -\sin\lambda & \cos\lambda & 0 \\ \cos\varphi\cos\lambda & -\cos\varphi\sin\lambda & \sin\varphi \end{pmatrix}\left(o\vec{q} - o\vec{v}\right) \tag{7}$$

The cosine of the view zenith angle is then given by the scalar product of u and (0,0,1) or

$$\cos\theta = \frac{u[3]}{\|u\|} \tag{8}$$

The azimuth angle α can be determined with ArcTan2 or ATAN2 function as

$$\alpha = ArcTan2\left(u[2], u[1]\right) \tag{9}$$

where care should be taken for u[1]=0 (observer on the equator). It should also be noted that the procedure by [4] is performing the calculation for a spherical rather than ellipsoidal Earth due to a small programming error. Furthermore this procedure does not make use of rotation matrices, and is less efficient.

APPENDIX B IMAGE GEOCODING

The scale relation between satellite scan angle and pixel position is given by the two relations [1]

$$c = COFF + round(x \bullet 2^{-16} \bullet CFAC) \tag{1}$$

where c indicates the column number

$$l = LOFF + round(y \bullet 2^{-16} \bullet LFAC) \tag{2}$$

where l indicates the line number
typical values for a full Earth disc image (bands 1 to 11) are e.g.

COFF=1856
LOFF=1856
CFAC=-13642337
LFAC=-13642337

These values mean in fact that the real size of a pixel at the nadir point is 3.00403165817 km for the bands 1-11, and 1.000134348869 km for HRV band 12. These values correspond respectively to angles of 83.8433 and 27.9478 μrad/pixel. Band 12 (HRV) is not considered further here.

The values of these parameters are retrieved from the header files. Parameters x and y are angles in degrees. The first problem is the forward projection. i.e. given (λ,ϕ) then determine (λ,ψ) (see also Fig. 3 and App. A)

$$\lambda = longitude \tag{3}$$

$$\psi = \arctan\left[\left(\frac{r_{pol}^2}{r_{eq}^2}\right)\tan(\varphi)\right] \tag{4}$$

where (λ,ϕ) are geographic coordinates (WGS84), and (λ,ψ) are geocentric coordinates .

Earth flattening 1/f=295.49. The distance dv from the satellite to the center of the Earth is 42142.5833 km (varying slightly).

When P is a point on the surface of the Earth, and r_e is the distance from P to the center then

$$r_e = \frac{r_{pol}}{\sqrt{1-\frac{r_{eq}^2 - r_{pol}^2}{r_{eq}^2}\cos^2(\psi)}} \tag{5}$$

We define further sub_lon as the longitude of the geostationary satellite (in the case of MSG-1 HRIT files this is 0)

Now we have

$$r_1 = dv - r_e\cos(\psi)\cos(\lambda - sub\_lon) \tag{6}$$

$$r_2 = -r_e\cos(\psi)\sin(\lambda - sub\_lon) \tag{7}$$

$$r_3 = r_e\sin(\psi) \tag{8}$$

$$r_n = \sqrt{r_1^2 + r_2^2 + r_3^2} \tag{9}$$

$$x = \arctan\left(\frac{-r_2}{r_1}\right) \tag{10}$$

$$y = \arcsin\left(\frac{-r_3}{r_n}\right) \tag{11}$$

Convert x and y into degrees and then insert these values into (1) and (2) to retrieve row and column number of the pixel.

The inverse projection assumes that we are given row and column number of a pixel in the image, and then have to determine (λ,ϕ). First, equations (1) and (2) will give values for x and y in degrees, which will then have to be converted to radians.

$$q^2 = \left(\frac{r_{eq}}{r_{pol}}\right)^2 \tag{12}$$

$$d^2 = dv^2 - r_{eq}{}^2 \tag{13}$$

Numeric values are q=1.006803 and d^2=1737121856

$$s_d = \sqrt{(dv\cos x\cos y)^2 - (\cos^2 y + q^2\sin^2 y)d} \tag{14}$$

$$s_n = \frac{dv\cos x\cos y - s_d}{\cos^2 y + q^2\sin^2 y} \tag{15}$$

$$s_1 = dv - s_n\cos x\cos y \tag{16}$$

$$s_2 = s_n\sin x\cos y \tag{17}$$

$$s_3 = -s_n\sin y \tag{18}$$

$$s_{xy} = \sqrt{s_1^2 + s_2^2} \tag{19}$$

$$\lambda = \arctan\left(\frac{s_2}{s_1}\right) + sub\_lon \tag{20}$$

$$\varphi = \arctan\left(q^2\frac{s_3}{s_{xy}}\right) \tag{21}$$

APPENDIX C RADIOMETRIC CORRECTION

First for all 12 bands offsets and gains need to be retrieved from the profile. Table 1 below shows some typical values obtained for the image of Aug. 5, 2004, 1200 hrs

Table 1 Slopes and offsets for the image Aug. 5, 2004, 1200 hrs. Band constants are given for use with visible and thermal channels. Unit conversion factors are $10/\lambda_0^2$.

				sensor	solar				
			cntral wvl	bndwdth	irrad	conv	for use with Planck's Law		
	slope	offset	m	m	Wm	$10/\lambda_0^2$		A	B
1	0.02295	-1.17046	0.635	0.0745	120.500	24.8000	NA	NA	NA
2	0.02922	-1.49001	0.810	0.0573	63.750	15.2416	NA	NA	NA
3	0.02328	-1.18724	1.640	0.1256	29.140	3.7180	NA	NA	NA
4	0.00366	-0.18659	3.900	0.5585	NA	0.6575	2569.09	0.9959	3.471
5	0.00832	-0.42422	6.250	0.8484	NA	0.2560	1598.57	0.9963	2.219
6	0.03862	-1.96972	7.350	0.4790	NA	0.1851	1362.14	0.9991	0.485
7	0.12674	-6.46392	8.701	0.3458	NA	0.1321	1149.08	0.9996	0.181
8	0.10396	-5.30202	9.660	0.2490	NA	0.1072	1034.35	0.9999	0.060
9	0.20503	-10.45676	10.800	0.9748	NA	0.0857	930.66	0.9983	0.627
10	0.22231	-11.33788	12.000	0.9373	NA	0.0694	839.66	0.9988	0.397
11	0.15761	-8.03795	13.400	1.2522	NA	0.0557	752.38	0.9981	0.576
12	0.03138	-1.60020	0.750	0.4220	591.260	17.7778	NA	NA	NA

$$L_{wn} = slope * DN + offset \tag{1}$$

The units of L_{wn} are $mWm^{-2}sr^{-1}(cm^{-1})^{-1}$. The units are in energy per wave number. This is done to bring the units in line with those of the GOES satellites. It should be noted that we can also write

$$L_{wn} = slope * (DN - 51) \tag{2}$$

The offset is equal to 51*slope for all channels

To convert the units from $mWm^{-2}sr^{-1}(cm^{-1})^{-1}$ into $Wm^{-2}sr^{-1}\mu m^{-1}$ the values for each channel have to be multiplied with $10/\lambda_0^2$ where λ_0 is the central wavelength in μm (values are given in Table 1).

To calculate reflectances from radiance the following relations are used

$$\rho_0 = \frac{\pi\, L_{wn} d_{SA}^{\,2} \Delta\lambda}{R_{TOA} \cos\theta} \tag{3}$$

where R_{TOA} is the solar radiance on top of the atmosphere (Wm^{-2}). L_{wn} should be expressed in the same units as R_{TOA}. If L is in $Wm^{-2}sr^{-1}\mu m^{-1}$ then Formula 3 is valid for R_{TOA} in Wm^{-2} as in Table 1. If L is in $mWm^{-2}sr^{-1}(cm^{-1})^{-1}$ then Eqn (3) should be changed using VIS06 20.76, VIS08 23.24, NIR16 19.85 and HRV 25.11 $mWm^{-2}sr^{-1}(cm^{-1})^{-1}$. Cosθ is the cosine of the solar zenith angle and d_{SA} is the Earth-Sun distance (J is Julian day) given by

$$d_{SA} = 1 - 0.0167 \cos\left(\frac{2\pi(J-3)}{365}\right) \tag{4}$$

The thermal channel radiances may be converted into brightness temperatures as follows (brightness temperatures are the temperatures derived from top-of-the-atmosphere radiances, so they do not take into account atmospheric corrections)

The equivalent brightness temperature of a satellite observation is defined as the temperature of a black body which emits the same amount of radiation as observed. Thus the brightness temperature follows from

$$R = \int_{\Delta\nu} \phi_\nu R_b(\nu, T_b) d\nu \Big/ \int_{\Delta\nu} \phi_\nu d\nu \tag{5}$$

with R the observed radiances in $mWm^{-2}sr^{-1}(cm^{-1})^{-1}$, R_b the Planck function and T_b the equivalent brightness temperature in K, ν wave number (in cm^{-1}) and ϕ the instrument spectral response. In the MSG documentation the following relation is adopted

$$R = \frac{c_1 \nu_c^3}{\exp[c_2 \nu_c / (AT_b + B)] - 1} \tag{6}$$

where ν_c is the central wave number (see also Table 1 for constants A and B and the central wave numbers) The radiation constants are given by $c_1=2hc^2$ and $c_2=hc/k_B$. c is the velocity of light, k_B is Boltzmann's constant and h is Planck's constant (see Table 2)

The inverse of this equation reads

$$T_b = \left[c_2 \nu_c \Big/ \log\left(c_1 \nu_c^3 \Big/ R + 1 \right) - B \right] \Big/ A \tag{7}$$

Table 2 Fundamental constants for use with Planck's Law and determination of brightness temperatures

physics.nist.gov constants

			error
c	2.997924580E+08	ms^{-1}	
h	6.626068760E-34	Js	520
kB	1.380650300E-23	JK^{-1}	2400
c1	1.191040000E-05	$mWm^{-2}sr^{-1}(cm^{-1})^{-4}$	
c2	1.438770000E+00	$(cm^{-1})^{-1}$	